

EXPERIMENTAL STUDY ON HEAT TRANSFER ENHANCEMENT OF FLUID FLOW INSIDE INTERNALLY FINNED PIPE BY THE USE OF MAGNETIC PARTICLE SUSPENSIONS IN PULSATING FLOW

Varut Emudom¹ and Apiwat Suyabodha²

¹Lecturer, Department of Mechanical Engineering, Rangsit University,
52/347 Phaholyothin Rd, Lak Hok, Muang District, Patumthani, 12000 Thailand,
varutama8008@gmail.com

²Lecturer, Department of Automotive Engineering, Rangsit University,
52/347 Phaholyothin Rd, Lak Hok, Muang District, Patumthani, 12000 Thailand,
apiwat.s@rsu.ac.th

ABSTRACT

The method for increasing the rate of heat transfer is presented in this experimental study using the suspensions of magnetic particles which are composed of γ -Fe₂O₃ magnetic particles (gamma-typed iron oxides) ranging in average diameter size 10-20 nm dispersed in distilled water. At different volume concentrations of 0.50%, 0.75%, 1% and 1.25%, the experiments were conducted in a vertical, internally finned pipe. To increase the heat transfer rate, three different intensities of external magnetic field 800 Gauss (G), 1,600 G, and 2,400 G were applied during the pipe flow experiments. All tests were performed within the Reynolds number ($Re \sim 2,900-9,800$). The outside surface area of the copper pipe was directly applied by the uniform surface heat flux during heat transfer experiments. As the volume concentration of the magnetic particles and the external magnetic field intensity increased, the average heat transfer coefficients increased. The maximum increase in heat transfer rate can be gained at particle volume concentration of 1.25% and the strength of external magnetic field of 2,400 G as compared to the base case with no application of the external magnetic field (0 G). The pulsating flow with high frequency is another factor which can increase the heat transfer rate in the pipe flow. At the frequency of 15 Hz, considerable amount of heat transfer rate can be attained.

KEYWORDS: gamma-typed iron oxides, surface heat flux, magnetic field, pulsating flow, heat transfer rate, average heat transfer coefficients

1. Introduction

Traditional heat transfer fluids such as oil and water with low thermal conductivity have limitations to improve the efficiency of many engineering equipment. To improve the performance of several engineering equipment that involve the heat transfer such as heat exchangers and electronic devices, heat transfer fluids with high thermal conductivity have been used. The use of very small magnetic particles as the dispersed phase to increase the thermal conductivity of the fluids is one of many innovative attempts. The average size of magnetic particles must be under 30 nm to be able to uniformly be suspended in a liquid. The solid volume concentration has a major effect on the magnetic particle suspensions' energy transport. The dramatic improvements in effective thermal conductivity have been indicated in many recent experiments [1, 2]. The ratio of magnetic particle suspensions' thermal conductivity with respect to pure water can be increased by increasing the magnitude of the applied magnetic field [3]. The magnetic particle suspensions' thermal conductivity can be increased exponentially with the particle volume concentration and the suspensions' temperature as reported by another researcher [4]. The heat transfer performance of magnetic particle suspensions in the vertical pipe flow has been reported by a few publications. For practical heat transfer processes in pipe flow, more studies are needed for using the magnetic particles as the dispersed phase.

The magnetic particle suspensions comprise of ferromagnetic particles as a dispersed phase and a nonmagnetic, continuous fluid [5]. Typically, the magnetic particles are very small in the range between 10 nm and 30 nm in diameter, which are coated with layers of surfactants to keep the particles uniformly and stably suspended in the carrier fluid [6]. The dipole-dipole interactions may cause the aggregation of some magnetic particles [7]. Without the externally applied magnetic field, the suspensions do not have any net magnetization and the magnetic particles are oriented randomly. When the suspensions are imposed by the external magnetic field, the magnetic particles in the suspensions align to form chain-like structural shapes in the same direction as the magnetic field [8]. The magnetic particle suspensions can be a major role for many heat transfer applications because the suspensions can be manually controlled by the temperature variation and magnitude of the externally applied magnetic field. The viscosity of magnetic particle suspensions was investigated to be used for applications in heating and cooling systems [9]. To improve high stability of the suspensions for increasing heat transfer performance, some dispersants such

as gum acaria and cetyl trimethyl ammonium chloride were investigated to be used in the suspensions [10]. Another experiment was done to determine the frequency of the oscillating applied field has effects on the variations of the local heat transfer coefficients [11]. Another interesting report was to determine the forced convection heat transfer in a pipe partially filled with the porous medium was affected by the magnetic field induced by a finite length solenoid [12]. A higher mixing intensity and breaking of the thermal boundary layer were results of the combined effects caused by the magnetic field and the porous medium. This in turn can optimize the enhancement of the local heat transfer coefficients and local Nusselt number values. The heat transfer characteristics were determined numerically by some investigators. A zigzag-shaped microchannels and a channel with sinusoidal walls were used as the models [13]. As shown in the studies, heat transfer can be increased in the sinusoidal microchannel without the use of any magnetic particles in the carrier fluid. Decreasing the wavelengths of sinusoidal and zigzag-shaped microchannels can cause the increasing in the local heat transfer coefficients. Some applications such as electronic cooling was investigated in two-phase closed thermosiphon filled with nanofluids [14].

In this study, the heat transfer performance by using the magnetic particle suspensions was investigated in the vertical, internally finned pipe. The fins' helix angle is 15° as compared to the other studies which were done with the helix angle more than 18° . The important parameters such as the particle volume concentrations, the magnitude of the external applied magnetic fields and the frequency of the pulsating flow were the main objectives of this study in order to find the right choices for heat transfer enhancement.

2. Objectives

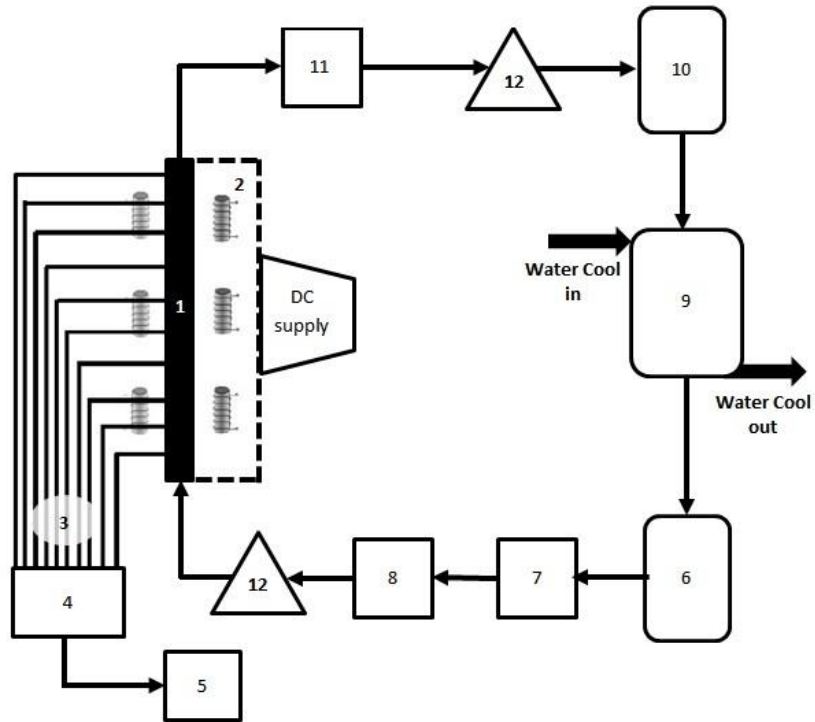
The objective of this study is to identify the important parameters such as the particle volume concentrations, the magnitudes of the external magnetic field, the frequency of the pulsating flow and internally finned pipe with have a major effect on heat transfer enhancement in the pipe flow.

3. Materials and methods

3.1 Apparatus

Figure 1 shows schematically an experimental apparatus for experiments in the vertical, internally finned pipe flow. The test system consists of a flow loop, a heated test section, a heat exchanger, solenoid coils, measuring and controlling units. Two types of pumps were used for testing. A Longer peristaltic pump which comprises of three rollers, silicone tube, inverter, and 0.75-hp AC motor was used for pulsating flow. A centrifugal pump was used for continuous flow. The surface of the copper, internally finned pipe was connected by ten thermocouples to measure the wall temperature at different locations. The cooling effect was done by using the heat exchanger to maintain a constant temperature of the magnetic particle suspensions at the inlet of the test section. Three pairs of solenoid coils were placed at the left and right side of the test section to generate the external magnetic field. A maximum current of 50 Amp from the DC power supply and maximum voltage of 150 V were used to produce the magnetic field. The external magnetic field was directed perpendicularly to the axial flow direction of the magnetic particle suspensions. Figure 2 shows the schematic diagram of the internally finned pipe. The details of internally finned pipe are shown in Table 1.

The test section included a straight, internally finned, copper pipe with 850 mm length, 9.2 mm inner diameter and 10.1 mm outer diameter. The uniform surface heat flux was imposed by wrapping the Nichrome wire around the test pipe. The Nichrome wire was then connected to a DC power supply with maximum power of 500 W. An aluminum foil and rubber were used as the insulation of the test pipe to prevent the heat transfer loss. The thermocouples number 1 to 10 were placed at these distances: 45 mm, 180 mm, 230 mm, 315 mm, 400 mm, 450 mm, 535 mm, 620 mm, 670 mm and 750 mm with respect to the tube inlet.



1	Finned pipe	5	Computer	9	Heat exchanger
2	Electromagnets	6	Reservoir tank	10	Overhead reservoir
3	Thermocouple wires	7	Pump	11	Separator
4	Data logger	8	Flow meter	12	Control valve

Figure 1 Schematic diagram of the experimental apparatus

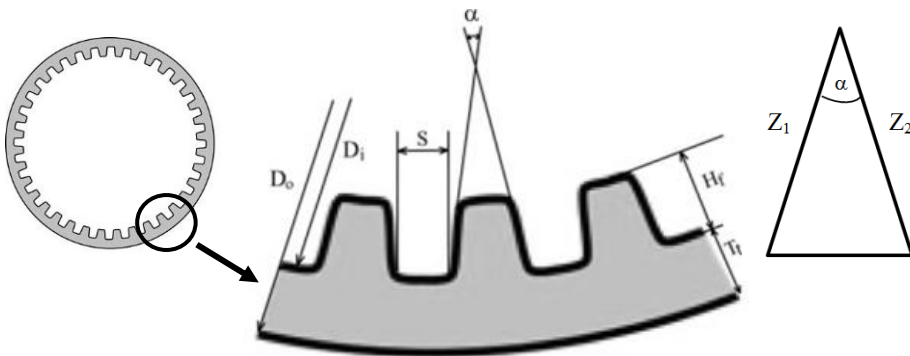


Figure 2 Schematic diagram of the internally finned pipe

Table 1 Specifications of the internally finned pipe

Parameters	Values
Inside diameter, D_i (mm)	9.2
Outside diameter, D_o (mm)	10.1
Tube thickness, T_t (mm)	0.45
Fin spacing, S (mm)	0.26
Fin height, H_f (mm)	0.125
Apex angle, α	55°
Number of fins	65
Tube length (mm)	850

3.2 Materials and preparation

In this study, the mixture of magnetic particles in the form of gamma-typed iron oxides Fe_2O_3 and distilled water were used as the magnetic particle suspensions. The important characteristics of the Fe_2O_3 iron oxides are known for their cubic cell structures and the moments of the individual atoms are aligned in the same direction [15]. The magnetic permeability constants of the particles are in the range between 0.5 to 35.5 and average size of 10-20 nm in diameters [15].

3.3 Data analysis

The total heat transfer rate for the entire pipe can be calculated by the following equation [16]

$$q_{conv} = mC_p (T_{m,exit} - T_{m,inlet}) \quad (1)$$

where q_{conv} is the total heat transfer rate, m is the mass flow rate of the suspensions and C_p is the specific heat.

The local heat transfer coefficient ($h(y)$) can be calculated from Newton's law of cooling as [16]

$$h(y) = (Q_{ave} / A_s) / [T_s(y) - T_m(y)] \quad (2)$$

where Q_{ave} / A_s is the uniform surface heat flux, T_s is the surface temperature along the copper pipe and T_m is the average temperature of the magnetic particle suspensions. The coordinate y is used as the vertical distance starting from $y = 0$ at the copper pipe inlet. Q_{ave} is the average heat transfer rate which can be calculated from

$$Q_{ave} = [IV + mC_p (T_{m,exit} - T_{m,inlet})] / 2 \quad (3)$$

where I is the measured current and V is the supplied voltage. From Equation (2), A_s is the inside heat transfer surface area of the internally finned pipe which can be calculated from

$$A_s = (Z_1 + Z_2 + S) \times \text{Number of fins} \times \text{Tube length} \quad (4)$$

The rate of change between the axial distance along the tube and the suspensions' average temperature can be expressed as the following equation [16]

$$dT_m / dy = q_s h (T_s - T_m) / (mA_s C_p) \quad (5)$$

The average temperature of the suspensions can be obtained by integrating the above expression from $y = 0$ at the tube inlet as following equation

$$T_m (y) = T_{m,inlet} + q_s y / mC_p L \quad (6)$$

where L is the total pipe length. Finally, the average values of convective heat transfer coefficients are calculated by integrating the local values of $h(y)$ for the entire pipe length ($y = 0$ to $y = L$) and dividing by the total pipe length

$$h_{avg} = \left[\int h(y) dy \right] / L \quad (7)$$

The Nusselt number, Nu is the dimensionless number used to describe the ratio of the average heat transfer coefficient to the thermal conductivity of the magnetic particle

suspensions. It can be written as $Nu = h_{avg} D / k$ where D is the equivalent inside diameter of the tube. Nu was used to determine the performance in heat transfer rate the entire pipe.

3.4 Uncertainty analysis

The uncertainty (σ) can occur from the errors of the experimental data. The heat flux, the surface temperature along the copper tube, the supplied voltage, the electric current and the distance between the thermocouples are among the collected data causing errors. The uncertainty of the local heat transfer coefficient is calculated as follows

$$\sigma_h = \pm \sqrt{\left(\frac{\partial h}{\partial q_s''} \sigma_{q_s''}\right)^2 + \left(\frac{\partial h}{\partial T_s} \sigma_{T_s}\right)^2 + \left(\frac{\partial h}{\partial T_m} \sigma_{T_m}\right)^2} \quad (8)$$

From Equations (3) and (6), the uncertainties of the average temperatures of the suspensions and the uniform surface heat flux are calculated as follows

$$\sigma_{T_m} = \pm \sqrt{\left(\frac{\partial T_m}{\partial T_{m,i}} \sigma_{T_{m,i}}\right)^2 + \left(\frac{\partial T_m}{\partial y} \sigma_y\right)^2} \quad (9)$$

$$\sigma_{q_s''} = \pm \sqrt{\left(\frac{\partial q_s''}{\partial I} \sigma_I\right)^2 + \left(\frac{\partial q_s''}{\partial V} \sigma_V\right)^2} \quad (10)$$

Table 2 summarizes the uncertainties of the measurements in this study.

Table 2 Uncertainty of the measurements

Quantity	Uncertainty
ΔL (m)	1×10^{-3}
ΔI (Amp)	0.1
ΔV (Volt)	0.1
ΔT_s ($^{\circ}C$)	0.2

The relative uncertainty of the local heat transfer coefficient is calculated as follows

$$U_h = \frac{\sigma_h}{h} = \pm \sqrt{\frac{1}{h^2} \left[\left(\frac{\partial h}{\partial q_s''} \sigma_{q_s''} \right)^2 + \left(\frac{\partial h}{\partial T_s} \sigma_{T_s} \right)^2 + \left(\frac{\partial h}{\partial T_m} \sigma_{T_m} \right)^2 \right]} \quad (11)$$

The relative uncertainty of the surface heat flux is calculated as follows

$$U_{q_s''} = \frac{\sigma_{q_s''}}{q_s''} = \pm \sqrt{\frac{1}{q_s''^2} \left[\left(\frac{\partial q_s''}{\partial I} \sigma_I \right)^2 + \left(\frac{\partial q_s''}{\partial V} \sigma_V \right)^2 \right]} \quad (12)$$

For all the measured cases, the uncertainty values have been calculated. The percentage uncertainty of the local heat transfer coefficient was calculated to be $\pm 2.85\%$.

4. Results

The effects of different intensities (0 – 2,400 G) of the external applied magnetic field on the suspensions' temperature profile for the pulsating flow with frequency of 10 Hz and 15 Hz at the volume concentration of 0.5% and 1.0% are shown in Figures 3-6, respectively.

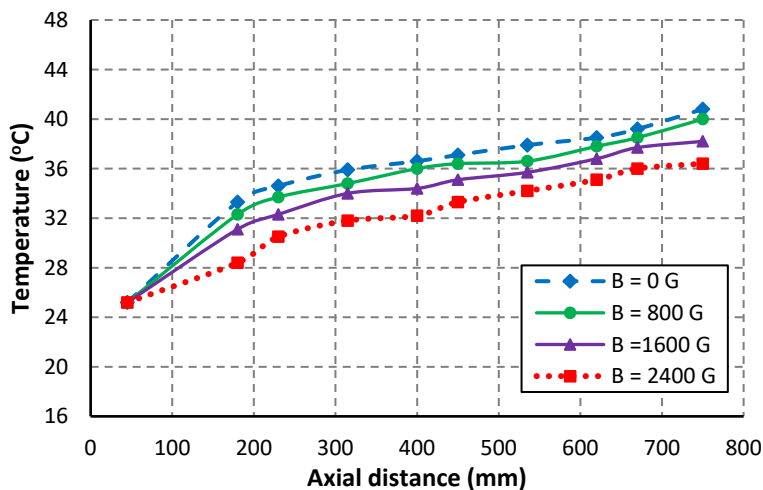


Figure 3 Effect of magnetic field on the suspensions' temperature at frequency of 10 Hz and 0.5% vol.

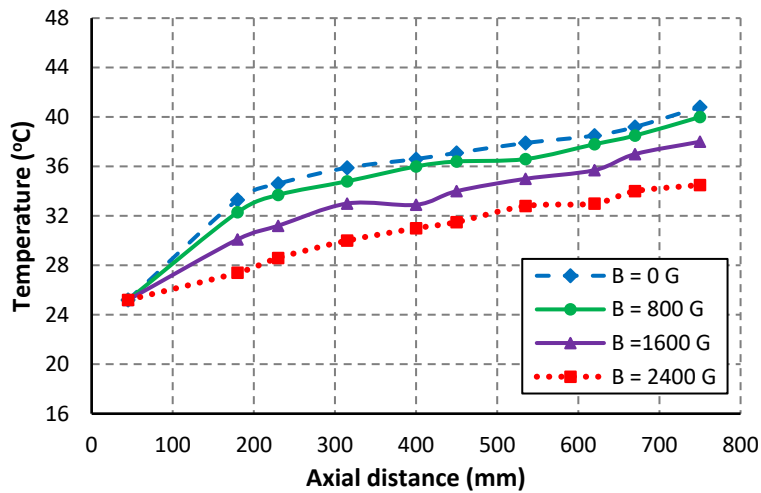


Figure 4 Effect of magnetic field on the suspensions' temperature at frequency of 10 Hz and 1.0% vol.

Figures 3 and 4 show the increase in temperature of the magnetic particle suspensions as the axial distance increases at different intensities of the external magnetic field. The pulsating flow was set at the frequency of 10 Hz.

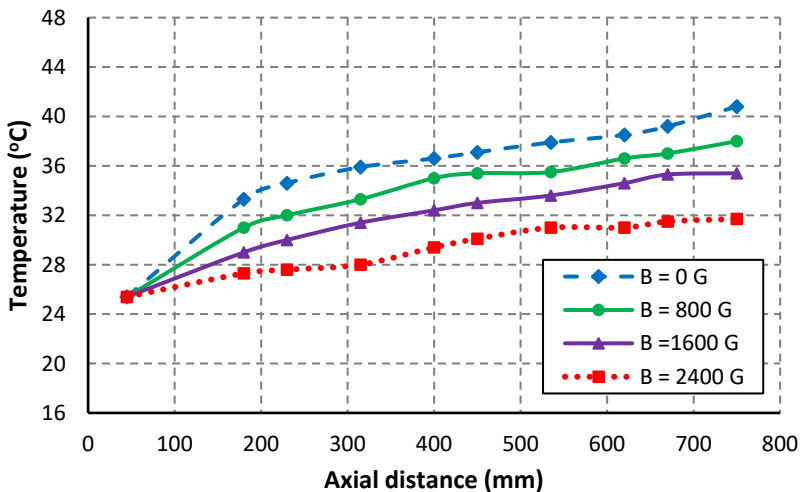


Figure 5 Effect of magnetic field on the suspensions' temperature at frequency of 15 Hz and 0.5% vol.

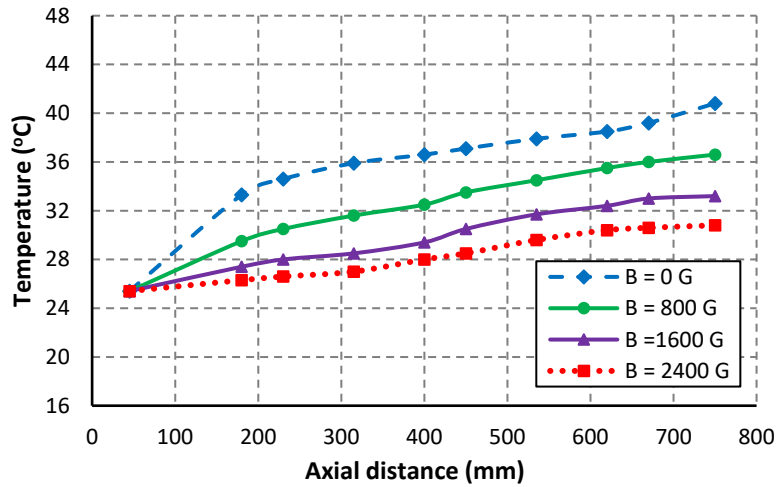


Figure 6 Effect of magnetic field on the suspensions' temperature at frequency of 15 Hz and 1.0% vol.

Figures 5 and 6 show the increase in temperature of the magnetic particle suspensions as the axial distance increases at different intensities of the external magnetic field. The pulsating flow was set at the frequency of 15 Hz.

By using the Nichrome wire to apply the constant surface heat flux over the copper, internally finned pipe, the suspensions' temperature had been remarkably decreased when the external magnetic field was applied to the flow of the suspensions. The suspensions' temperature decreased when the particle volume concentrations increased. Comparing the case with no application of the external magnetic field, the decrease in temperature of 9.5°C could be obtained for the external magnetic field with an intensity of 2,400 G, the particle volume concentration of 1.0% and at the frequency of 15 Hz in pulsating flow. Figures 7 and 8 present the local heat transfer coefficients as a function of relative axial distance starting from the pipe inlet at volume concentration of 1.0% in pulsating flow at frequency of 10 Hz and 15 Hz, respectively.

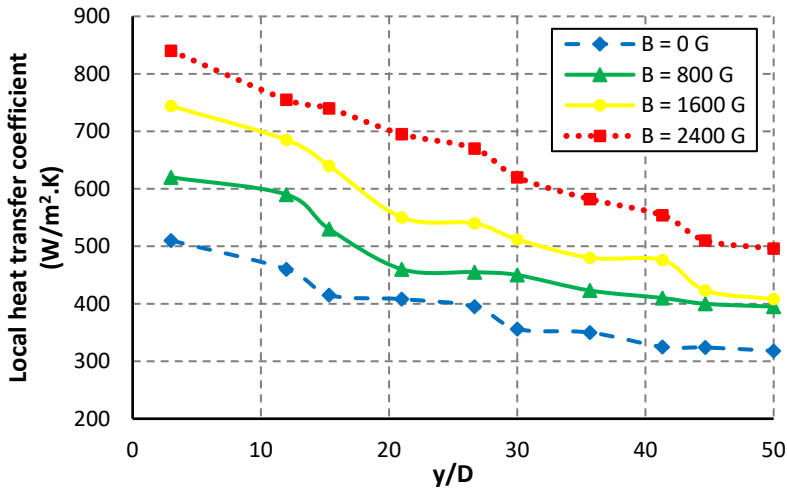


Figure 7 Profile of the local heat transfer coefficients at frequency of 10 Hz and 1.0% vol.

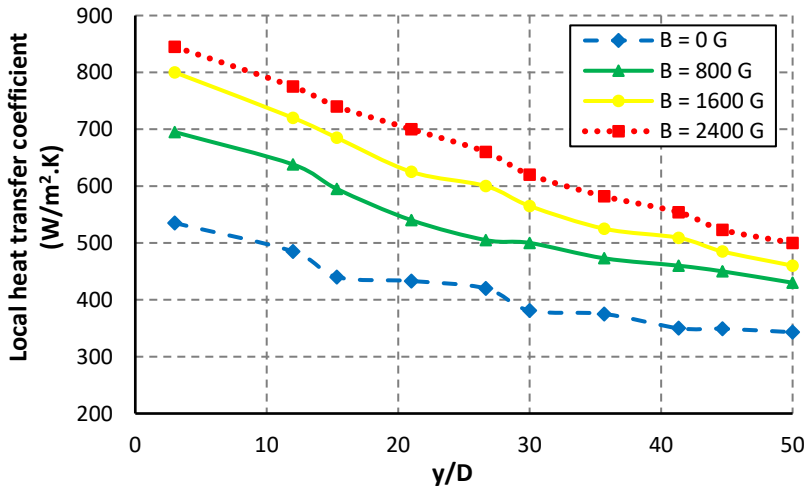


Figure 8 Profile of the local heat transfer coefficients at frequency of 15 Hz and 1.0% vol.

Figures 7 and 8 show the decreasing of the local heat transfer coefficients with the increasing in the axial distance of the pipe. The heat transfer enhancement could not perform well for the magnetic particle suspensions without applying an external magnetic field to the flow, hence low numbers for the local heat transfer coefficients. With the increasing axial distance starting from the entrance to the exit of the copper pipe, values of the local heat transfer coefficient, $h(y)$ decreased. The local heat transfer coefficients increased as the particle volume concentrations increased. As expected, an intensive performance of heat

transfer could be acquired by applying a stronger magnetic field. Figures 9 and 10 show that the average values of convective heat transfer coefficient increase as the volume concentration of magnetic particles and Reynolds number increase. Four different volume concentration of 0.50%, 0.75%, 1.00% and 1.25% are shown with two different frequencies (10 Hz and 15 Hz) of pulsating flow.

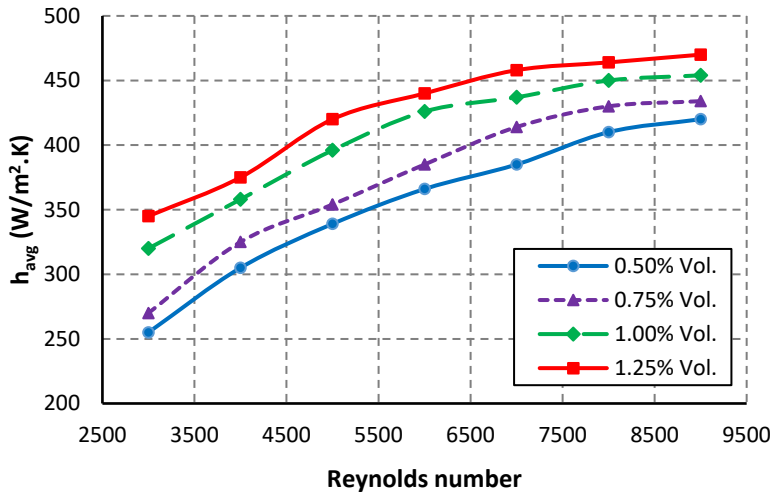


Figure 9 Average heat transfer coefficient as a function of the Reynolds number at 10 Hz

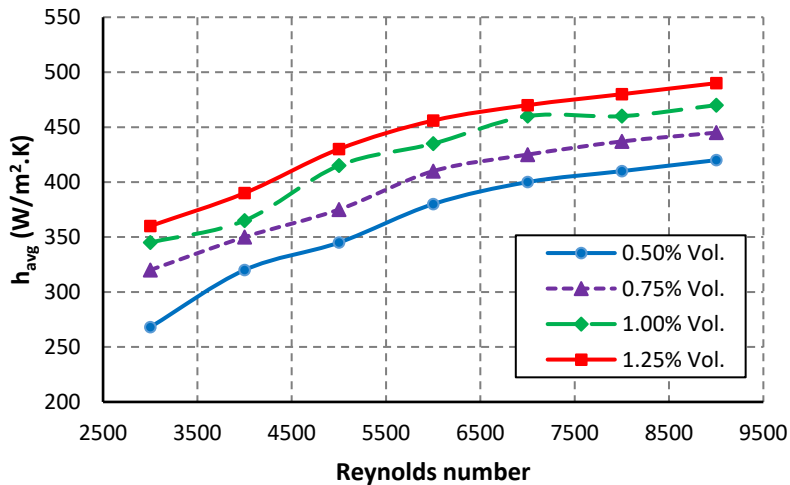


Figure 10 Average heat transfer coefficient as a function of the Reynolds number at 15 Hz

The relationship between the Nusselt number and the Reynolds number is shown in Figure 11 for the continuous flow and the pulsating flow with the frequencies of 10 Hz and 15 Hz. The volume concentration of magnetic particles is 1.0% and the intensity of external magnetic field of 2,400 G.

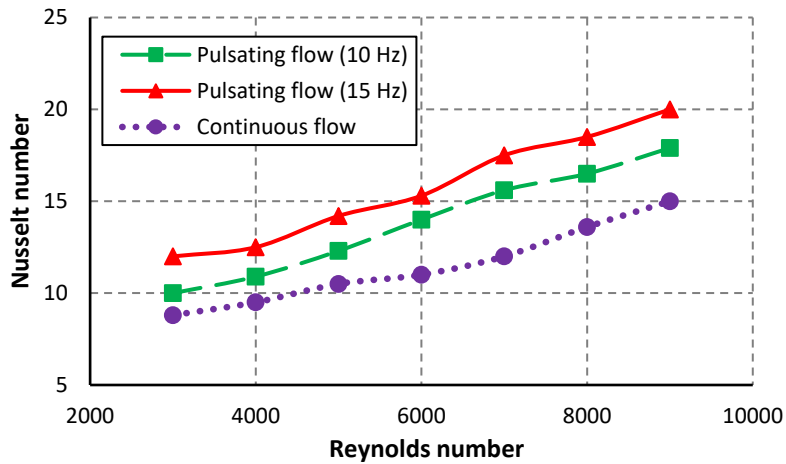


Figure 11 Profile of Nusselt number and Reynolds number at magnetic field of 2,400 G and volume concentration of 1.0%

Figure 11 shows the increase in the Nusselt number, hence, the increase in heat transfer as the flow frequency increases. The Nusselt number with higher frequency pulsating flow show higher than lower ones. The frequency pulsating flow has major effect on the Brownian motion of suspending magnetic particles in the base fluid which results in higher disturbance in the main suspensions flow. Therefore, the suspensions with higher pulsating frequency are likely to enhance more heat transfer than the continuous flow. The other interesting explanations of the performance in heat transfer from this experiment. The decreasing of the local heat transfer coefficients with the increasing of the axial distance is caused by the growth of the thermal boundary layer. However, the magnetic particle suspensions can be used to increase the average heat transfer coefficients. The convective heat transfer can be improved by increasing the volume concentration of magnetic particles. Without application of the external magnetic field, the magnetic moments within the magnetic particles are oriented randomly. The magnetic particles are affected mainly by the Brownian motion in which the thermal energy is greater than the magnetic dipolar energy [17]. The

Brownian motion is the random motion of very small particles suspended in a carrier liquid. When the external magnetic field is applied to the magnetic particle suspensions, the magnetic dipolar energy becomes stronger and can overcome the thermal energy [18]. The magnetic moments adjust magnetic particles to align themselves in direction of the external magnetic field forming some agglomerates and many short chain-like structural shapes. The formation of magnetic particles in chain-like structures increases as the strength of magnetic field increases. The linear chain-like structures become longer when the volume concentration of magnetic particles is increased, hence the heat transfer can perform remarkably well. Also, increasing the thermal conductivity of the suspensions can enhance the forced convective heat transfer. The main mechanism of suspensions' thermal conductivity is the magnetic torque that aligns the magnetic moments of the magnetic particles in direction of the external magnetic field. Therefore, increasing the thermal conductivity of the suspensions can be attained by increasing the strength of the external magnetic field, hence, the heat transfer enhancement can be increased.

5. Conclusions

The performance in heat transfer of the magnetic particle suspensions of iron oxides Fe_2O_3 was investigated experimentally in a copper, internally finned pipe. The performance in heat transfer was improved by imposing the external magnetic field to the magnetic particle suspensions. The experiments showed that the average heat transfer coefficients increased with the increasing the volume concentration of magnetic particles and the strength of the external magnetic field. Also, the internally finned pipe can optimize the convective heat transfer better than the ordinary round pipe. As compared with the continuous flow, the pulsating flow can considerably affect the heat transfer enhancement. The high frequency flow can be a major reinforcement to help increasing the heat transfer rate within pipe flow.

References

- [1] Esfe MH, Raki HR, Emami MRS, Afrand M. Viscosity and rheological properties of antifreeze base nanofluid containing hybrid nano-powders of MWCNTs and TiO_2 under different temperature conditions. Powder Technology 2019;342:808-16. doi: 10.1016/j.powtec.2018.10.032.

- [2] Jeong J, Li C, Kwon Y, Lee J, Kim S H, Yun R. Particle shape effect on the viscosity and thermal conductivity of ZnO nanofluids. *International Journal of Refrigeration* 2013;36(8):2233-41.
- [3] Karimi A, Goharkhah M, Ashjaee M, Shafii M B. Thermal conductivity of Fe_2O_3 and Fe_3O_4 magnetic nanofluids under the influence of magnetic field. *International Journal of Thermophysics* 2015;36(10):2720-39. doi: 10.1007/s10765-015-1977-1.
- [4] Hojjat M, Etemad S, Bagheri R, Thibault J. Thermal conductivity of non-Newtonian nanofluids experimental data and modeling using neural network. *International Journal of Heat and Mass Transfer* 2011;54(5-6):1017-23. doi: 10.1016/j.ijheatmasstransfer.2010.11.039.
- [5] Zhou J, Gu G, Meng X, Shao C. Effect of alternating gradient magnetic field on heat transfer enhancement of magnetorheological fluid flowing through microchannel. *Applied Thermal Engineering* 2019;150:1116-25. doi: 10.1016/j.applthermaleng.2019.01.057.
- [6] Liou TM, Wei TC, Wang CS. Investigation of nanofluids on heat transfer enhancement in a louvered microchannel with lattice Boltzmann method. *Journal of Thermal Analysis and Calorimetry* 2019;135:751-62. doi: 10.1007/s10973-018-7299-3.
- [7] Khodadadi H, Toghraie D, Karimipour A. Effects of nanoparticles to present a statistical model for the viscosity of MgO-water nanofluid. *Powder Technology* 2019; 342: 166-180. doi: 10.1016/j.powtec.2018.09.076.
- [8] Arabpour A, Karimipour A, Toghraie D. The study of heat transfer and laminar flow of kerosene/multi-walled carbon nanotubes (MWCNTs) nanofluid in the microchannel heat sink with slip boundary condition. *Journal of Thermal Analysis and Calorimetry* 2018;131(2):1553-66. doi: 10.1007/s10973-017-6649-x.
- [9] Bahiraei M, Hangi M. Flow and heat transfer characteristics of magnetic nanofluids: a review. *Journal of Magnetism and Magnetic Materials* 2015;374:125-38. doi: 10.1016/j.jmmm.2014.08.004.
- [10] Sun B, Lei W, Yang D. Flow and convective heat transfer characteristics of Fe_2O_3 -water nanofluids inside copper tubes. *International Communication of Heat and Mass Transfer* 2015;64: 21-8. doi: 10.1016/j.icheatmasstransfer.2015.01.008.
- [11] Yarahmadi M, Goudarzi H M, Shafii M B. Experimental investigation into laminar forced convective heat transfer of ferrofluids under constant and oscillating magnetic field with different magnetic field arrangements and oscillation modes. *Experimental Thermal and Fluid Science* 2015;68:601-11. doi: 10.1016/j.expthermflusci.2015.07.002.

- [12] Fadaei F, Shahrokhi M, Dehkordi A M, Abbasi Z. Forced-convection heat transfer of ferrofluids in a circular duct partially filled with porous medium in the presence of magnetic field. *Journal of Magnetism and Magnetic Materials* 2019;475:304-15. doi: 10.1016/j.jmmm.2018.11.032.
- [13] Toghraie D, Abdollah M, Pourfatta F, Akbari O, Ruhani B. Numerical investigation of flow and heat transfer characteristics in smooth, sinusoidal and zigzag-shaped microchannel with and without nanofluid. *Journal of Thermal Analysis and Calorimetry* 2018;131(2):1757-66. doi:10.1007/s10973-017-6624-6.
- [14] Rashidi MM, Nasiri M, Khezerloo M, Laraqi N. Numerical investigation of magnetic field effect on mixed convection heat transfer of nanofluid in a channel with sinusoidal walls. *Journal of Magnetism and Magnetic Materials* 2016;401:159-68. doi: 10.1016/j.jmmm.2015.10.034.
- [15] Rosensweig RE. *Ferrohydrodynamics*. USA: Dover Publications, Inc.; 1997.
- [16] Incropera FP, Dewitt DP. *Introduction to Heat Transfer*. USA: John Wiley & Sons; 1996.
- [17] Keyvani M, Afrand M, Toghraie D, Reiszadeh M. An experimental study on thermal conductivity of cerium oxide/ethylene glycol nanofluid: developing a new correlation. *Journal of Molecular Liquids* 2018;266:211-7. doi: 10.1016/j.molliq.2018.06.010.
- [18] Meyer JP, Adio SA, Sharifpur M, Nwosu PN. The viscosity of nanofluids: a review of the theoretical, empirical and numerical models. *Heat Transfer Engineering* 2016;37(5):387-421. doi: 10.1080/01457632.2015.1057447.

Author's Profile



Varut Emudom received Ph.D. in Mechanical Engineering from the University of Illinois, U.S.A. in 2003. He is now with the Department of Mechanical Engineering at Rangsit University, Thailand. His main research interests include fluid mechanics, thermodynamics and heat transfer.



Apiwat Suyabodha received the Ph.D. in Automotive Engineering from University of Bath, United Kingdom. Currently, he is a lecturer in Automotive and Mechanical Engineering, Rangsit University, Thailand. His research interests focus on strength of material, combustion engine, dynamics of vehicles and simulation of engine.

Article History:

Received: June 19, 2023

Revised: November 8, 2023

Accepted: December 15, 2023